ELSEVIER

Journal of Power Sources 96 (2001) 90–93

JOURNAL OF POWER SOURCES

www.elsevier.com/locate/jpowsour

Electrocatalytic characteristics of the metal hydride electrode for advanced Ni/MH batteries

M. Geng[a], F. Feng[a], S.A. Gamboa[b], P.J. Sebastian[b], A.J. Matchett[c], D.O. Northwood[d,*]

[a]*Mechanical, Automotive & Materials Engineering, University of Windsor, Windsor, Ont., Canada N9B 3P4*
[b]*Centro de Investigacion en Energia-UNAM 62580 Tomixco, Morelos, Mexico*
[c]*Chemical Engineering, Tees-side University of Middlesbrough, Middlesbrough TS1 3BA, UK*
[d]*Faculty of Engineering and Applied Science, Ryerson Polytechnic University, 350 Victoria Street, Toronto, Ont., Canada M5B 2K3*

Received 13 November 2000; accepted 28 November 2000

Abstract

The electrocatalytic characteristics of a metal hydride (MH) electrode for advanced Ni/MH batteries include the hydrogen adsorption/desorption capability at the electrode/electrolyte interface. The hydrogen reactions at the MH electrode/electrolyte interface are also related to factors such as the surface area of the MH alloy powder and the nature of additives and binder materials. The high-rate discharge capability of the negative electrode in a Ni/MH battery is mainly determined by the mass transfer process in the bulk MH alloy powder and the charge transfer process at the interface between the MH alloy powder and the electrolyte. In this study, an AB_5-type hydrogen-absorbing alloy, Mm (Ni, Co, Al, Mn)$_{5.02}$ (where Mm denotes Mischmetal, comprising 43.1 wt.% La, 3.5 wt.% Ce, 13.3 wt.% Pr and 38.9 wt.% Nd), was used as the negative MH electrode material. The MH electrode was charged and discharged for up to 200 cycles. The specific discharge capacity of the alloy electrode decreases from a maximum value of 290–250 mAh g^{-1} after 200 charge/discharge cycles. A cyclic voltammetry technique is used to analyze the charge transfer reactions at the electrode/electrolyte interface and the hydrogen surface coverage capacity.

Keywords: Hydrogen-absorbing alloy; Metal hydride electrode; Hydrogen surface coverage; Cyclic voltammetry

1. Introduction

The use of metal hydrides (MH) as active negative electrode material in rechargeable alkaline Ni/MH batteries has been studied for some time. Although Ni/MH batteries have superior specific energy than the other two aqueous electrolyte systems (lead-acid and Ni/Cd batteries), they remain largely inferior to the new rechargeable lithium (Li-ion) batteries. However, lithium batteries are much more expensive to produce [1]. In addition, lithium batteries cannot be operated for a safety reasons without electronic control of each individual cell.

The reaction mechanism of hydrogen in a Ni/MH battery is similar to that of lithium in a Li-ion battery. Both H and Li atoms shuttle between the anode and cathode. We have reported a reaction model for hydrogen which shuttles between the anode and cathode in Ni/MH batteries [2,3]. Based on this shuttling model of hydrogen, Vassal et al. [4] have developed a rechargeable Ni/MH battery which uses an alkaline solid polymer electrolyte. The reaction processes for hydrogen and lithium in Ni/MH and Li-ion batteries are summarized in Table 1.

Hydrogen diffusion in the MH electrode dominates the high-rate discharge capability of the MH electrode in Ni/MH batteries. We have reported that the MH alloy powder in a Ni/MH battery will be stabilized after about 30 charge/discharge cycles [2]. The microcracking of the MH alloy powder on charge/discharge can lead to an increase in the specific reaction area. This also leads to an improvement in the charge transfer capability at the interface between the MH particles and the electrolyte.

During the discharge process, hydrogen diffuses from the interior of the bulk alloy to the surface of the alloy powder. This is the mass-transfer process. Also, hydrogen combines with OH^- ion to form H_2O at the electrode/electrolyte interface. This is the charge-transfer process. The anodic polarization performance of an alloy electrode is related to both the oxidation of the alloy powder (without hydrogen in the alloy) and the hydrogen diffusion from the interior to the surface of the alloy powder (with hydrogen in the alloy).

* Corresponding author. Tel.: +1-416-979-5102; fax: +1-416-979-5308.
E-mail address: dnorthwo@acs.ryerson.ca (D.O. Northwood).

0378-7753/01/$ – see front matter
PII: S0378-7753(00)00672-8

Table 1
Hydrogen and lithium diffusion processes in Ni/MH and Li-ion batteries [5]

Battery	Negative electrode	Electrolyte	Positive electrode
Ni/MH	$MH \underset{charge}{\overset{discharge}{\rightleftarrows}} M$	H^+	$NiO_2H \underset{charge}{\overset{discharge}{\rightleftarrows}} NiO_2H_2$
Li-ion	$C_6Li \underset{charge}{\overset{discharge}{\rightleftarrows}} C_6$	Li^+	$NiO_2 \underset{charge}{\overset{discharge}{\rightleftarrows}} NiO_2Li$

In this paper, we have studied the charge/discharge characteristics of a Mm (Ni, Co, Al, Mn)$_{5.02}$ (where Mm denotes Mischmetal, comprising 43.1 wt.% La, 3.5 wt.% Ce, 13.3 wt.% Pr and 38.9 wt.% Nd) alloy electrode. In particular, we have examined the charge transfer reactions at the electrode/electrolyte interface using a cyclic voltammetry technique.

2. Experimental

A hydrogen storage alloy of nominal composition Mm (Ni, Co, Al, Mn)$_{5.02}$ was prepared by induction melting and rapid cooling. The alloy ingot was mechanically pulverized to obtain a sifted particle size of 45–53 μm (the alloy powder was captured between 325 (45 μm) and 270 mesh (53 μm) sieves). The sifted alloy powder was used as the negative electrode material in an experimental cell. The positive electrode in this cell, a sintered Ni(OH)$_2$/NiOOH plate, was obtained from a commercial supplier.

The set-up of the experimental cells was in a sintered glass apparatus with three compartments. The negative electrode was placed in the central compartment and two Ni(OH)$_2$/NiOOH electrodes were placed on either side. For the specific capacity and exchange current density measurements, the MH alloy powders were mixed with nickel powder in a weight ratio of 1:1 together with a small amount (3 wt.%) of polytetrafluoroethylene (PTFE) aqueous solution as a binder and then pressed at a pressure of 500 MPa. The capacity of the positive electrode plates was designed to be higher than that of the negative electrode. An amount of 0.1 g of the alloy powder was separately used to make the negative electrode plates for two experimental cells. The electrolyte in the cells was a 6 M KOH aqueous solution [6].

The charge/discharge and polarization tests of the experimental cells were conducted using a Solartron 1285 Potentiostat with CorrWare software for Windows. The testing resolution of the potential, current and time is 0.1 mV, 0.1 mA and 0.1 s, respectively. The charge and discharge regimes were conducted at temperatures ranging from 273 to 335 K. The experimental cells were charged at a current of 100 mA g^{-1} for 3.2 h. and discharged at a current of 100–600 mA g^{-1} to an end-of-discharge-potential of −0.5 V versus Hg/HgO. Cycle voltammograms (CVs) were obtained at the scan rates ranging from 100 to 800 mV s^{-1}. The scanning potential was in the range from −1.1 to 0 V versus Hg/HgO. An interruption of electrode current was used to compensate for IR potential drop errors. The resistance of the electrolyte between the working electrode and the reference electrode, and the contact resistance are common causes of these errors.

3. Results and discussion

The active anode and cathode electrode materials for the rechargeable Ni/MH batteries are the hydrogen-absorbing alloys and nickel hydroxide compounds, respectively. The hydrogen-absorbing alloy, that have been developed in our group for the anode, was based on a $MmNi_5$-based alloy with partial replacement of Ni by Co, Mn and Al. It should be noted that the addition of Mn was used to increase the crystal cell volume, and to achieve an increase in specific capacity and better high-rate dischargeability. Adjustment of the stoichiometric composition of the $AB_{5+\delta}$ alloy is used to increase the anti-pulverization capability.

In the KOH aqueous solution, the standard redox potentials of the rare earth elements, Al and Mn range from −1.37 to −1.05 V versus SHE. These metallic elements are easily oxidized to form stable metal oxide compounds at the surface of the alloy powder. These oxides, as passivation phases, are used both to prevent further oxidation of the MH alloy powder, and to increase the charge/discharge cycle lifetime. However, the oxides at the powder surface lead to a decrease in the electrocatalytic activity [6].

Fig. 1 shows the discharge capacity of the Mm (Ni, Co, Al, Mn)$_{5.02}$ alloy electrode at different discharge currents. The discharge capacity at a 100 mA g^{-1} discharge current reaches 290 mAh g^{-1} during five charge/discharge cycles. The specific discharge capacity at a 600 mA g^{-1} discharge current reaches a value of 248 mAh g^{-1}. The MH electrode was charged/discharged over 200 cycles and the specific discharge capacity at a 100 mA g^{-1} discharge current remains at 250 mAh g^{-1} at 298 K. Generally, the manufacturing of the electrode, additives and bonding materials

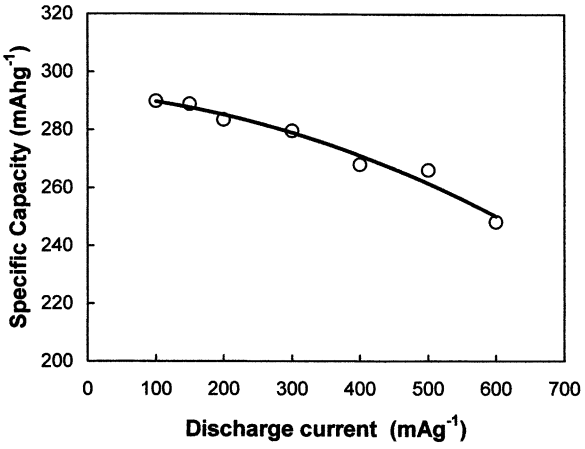

Fig. 1. Variation of specific capacity of Mm (Ni, Co, Al, Mn)$_{5.02}$ alloy electrode with discharge current.

slightly influence the specific discharge capacity, especially the high-rate discharge capability, because of the electrode swelling and an increase in the electrode resistance.

Fig. 2 shows the specific discharge capacity versus temperature plot. The discharge capacity was measured at a 100 mA g^{-1} discharge current. The specific capacity has a maximum value of 290 mAh g^{-1} at 298 K. The discharge capacity decreases to 252 mAh g^{-1} at 273 K and 246.4 mAh g^{-1} at 335 K. The electrochemical reaction at the surface of the MH alloy powder is controlled by the charge transfer process at the MH electrode/electrolyte interface and the mass transfer process in the bulk MH alloy. A higher temperature leads to both faster charge transfer and mass transfer reactions. However, the higher temperature also leads to a decrease in the hydrogen storage capacity in the MH alloy. The balance of these two factors leads to a maximum specific capacity at 298 K.

The equilibrium potential is a measure of the H^+ activity at the electrode/electrolyte interface. The equilibrium potential of Mm (Ni, Co, Mn, Al)$_{5.02}$ alloy as a function of the number of cycles and hydrogen storage capacity is shown in Fig. 3. The equilibrium potential does not change with increasing number of cycles for hydrogen storage capacities >60 mAh g^{-1}. However, at hydrogen storage capacities <60 mAh g^{-1}, the equilibrium potential increases with increasing number of cycles. The instability of the equilibrium potential at a lower hydrogen storage capacity could lead to instability for Ni/MH batteries after a large number of cycles.

The discharge Coulombic capacity (Q) of a metal-hydride electrode, obtained electrochemically as a function of the applied overpotential (E) in the cycle voltammograms, involves three components, namely:

1. A capacity (Q_C) due to the release of the absorbed hydrogen from the interior bulk to the surface of the alloy powder. The hydrogen released from the interior of the alloy powder leads to concentration polarization. Thus, the polarization current density from the concentration polarization is dependent on the scan rate for low scan-rate polarization measurements (for example, <100 mV s^{-1} scan rate).
2. A capacity (Q_A) due to the activation polarization reaction. The activation polarization current density is strongly dependent on the scan rate for higher scan-rate polarization measurements (for example, >200 mV s^{-1}).
3. A capacity (Q_S) from the hydrogen surface coverage in the alloy powder. This capacity is dependent on both the hydrogen surface coverage and the surface area. Because of a very fast reaction rate, the capacity due to the hydrogen surface coverage is independent of the scan rate.

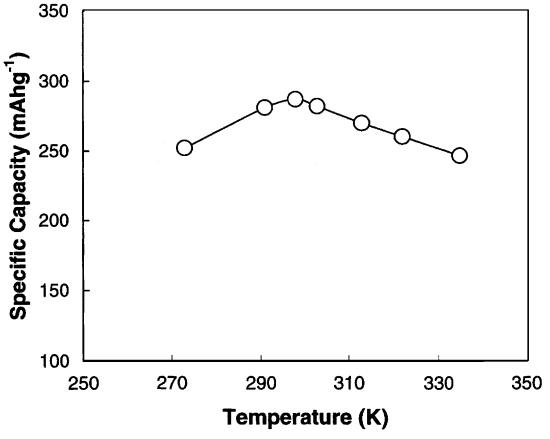

Fig. 2. Variation of specific capacity of Mm (Ni, Co, Al, Mn)$_{5.02}$ alloy with temperature.

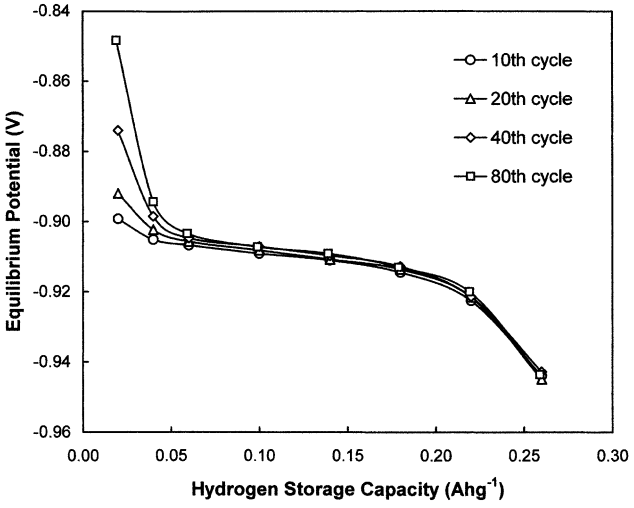

Fig. 3. Equilibrium potential of Mm (Ni, Co, Al, Mn)$_{5.02}$ electrode vs. hydrogen storage capacity at varying number of charge/discharge cycles.

The Coulombic capacity of the electrode, obtained from the CV technique, can be separated into the scan-rate-dependent activation and concentration capacities ($Q_A(v)$ and $Q_C(v)$) and the scan-rate-independent capacity (Q_S). Thus, the Coulombic capacity (Q) can be expressed as follows:

$$Q(v) = Q_C(v) + Q_A(v) + Q_S \quad (1)$$

and

$$Q_S = nFA\Gamma \quad (2)$$

where, A is the reaction surface area of the electrode and Γ the hydrogen surface coverage. The activation-related capacity is inversely proportional to scan rate, which can be approximately expressed as follows:

$$Q(v) = \int_{E_1}^{E_2} i(E)\mathrm{d}t = \gamma(E_1, E_2)\frac{1}{v} \quad (3)$$

where $i(E)$ is the anodic polarization current density and $\gamma(E_1, E_2)$ is obtained using a equation: $E = E_1 + vt$. The Coulombic capacity is calculated from anodic polarization current density in the potential range between E_1 and E_2.

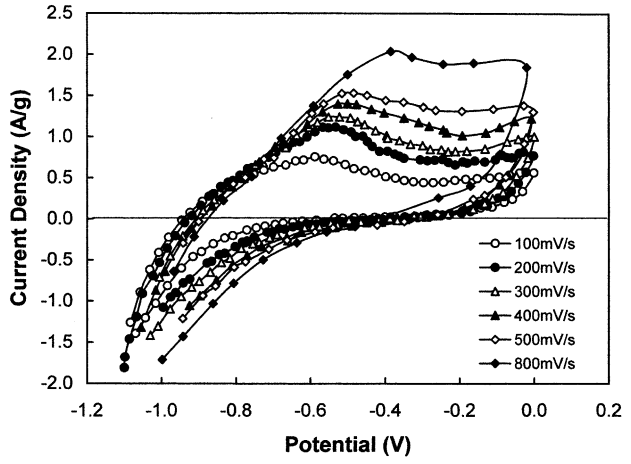

Fig. 4. Cycle voltammograms of a Mm (Ni, Co, Al, Mn)$_{5.02}$ alloy electrode at scan rates ranging from 100 to 800 mV s^{-1}.

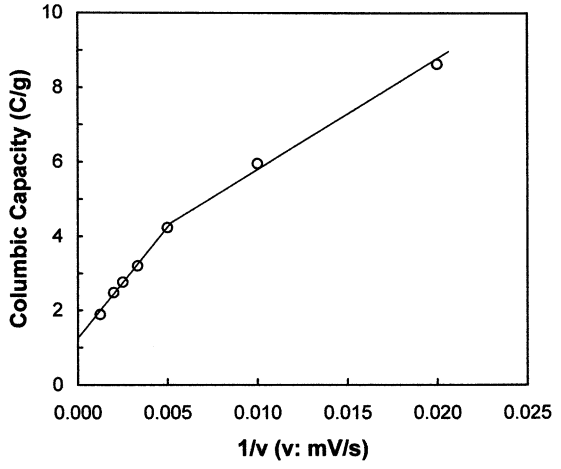

Fig. 5. Coulombic capacity of Mm (Ni, Co, Al, Mn)$_{5.02}$ alloy electrode for the anodic polarization process ($E_2 = 0$ V) vs. the inverse of the scan rate.

Fig. 4 shows cyclic voltammograms at scan rates ranging from 100 to 800 mV s^{-1}. The value of peak anodic current density, as seen in Fig. 4, is influenced by the hydrogen release from the interior of the alloy powder at a low scan rate (<200 mV s^{-1}) i.e. the concentration polarization current density. The anodic current density mainly results from the activation reaction at high scan rates (>200 mV s^{-1}) and hydrogen diffusion from the interior into surface of the alloy powder has only small influence on the anodic current density for high scan-rate polarization. The hydrogen surface coverage capacity can be determined at a sufficiently high scan rate. The Coulombic capacity is plotted in Fig. 5 against the inverse of the scan rate for the anodic polarization period ($E_2 = 0$ V). The hydrogen surface coverage capacity, Q_S, at the surface of the MH electrode, was estimated to be about 1.2 C g^{-1} by extrapolation of the Coulombic capacity versus 1/v plot. The value of the hydrogen surface coverage relates to the electrocatalytic characteristics at the electrode/electrolyte interface.

4. Conclusions

The main conclusions from this study are:

1. The discharge capacity of a Mm (Ni, Co, Al, Mn)$_{5.02}$ electrode at 298 K remains stable at 250 mAh g^{-1} after 200 cycles.
2. The specific discharge capacity of the MH electrode reaches a maximum value at 298 K and the specific capacity decreases to 252 mAh g^{-1} at 273 K and 246.4 mAh g^{-1} at 335 K.
3. The activation-related capacity, obtained from CVs, is inversely proportional to the scan rate. The Coulombic capacity from hydrogen surface coverage is independent of the scan rate. The hydrogen surface coverage capacity in this electrode, was estimated to be 1.2 C g^{-1} by extrapolation of the Coulombic capacity versus 1/v plot.
4. The instability of the equilibrium potential at a lower hydrogen storage capacity could lead to instability in Ni/MH batteries after a large number of cycles.

Acknowledgements

Funding for this work is being provided by the Natural Science and Engineering Research Council of Canada through a Research Grant (A4391) awarded to Professor Derek O. Northwood.

References

[1] P. Ruetschi, F. Meli, J. Desilvestro, J. Power Sources 57 (1995) 85.
[2] M. Geng, J. Han, F. Feng, D.O. Northwood, Int. J. Hydrogen Energy 23 (1998) 1055.
[3] M. Geng, J. Han, D.O. Northwood, in: Proceeding of the 2nd International Symposium on New Materials for Fuel Cell and Modern Battery Systems, Montreal, Que., Canada, 1997, p. 585.
[4] N. Vassal, E. Salmon, J.-F. Fauvarque, J. Electrochem. Soc. 146 (1999) 20.
[5] G. Benczur-Urmossy, D. Ohms, M. Berthold, K. Wiesener, Electrochem. Soc. Proc. (ESC) 97-18 (1997) 812.
[6] M. Geng, J. Han, F. Feng, D.O. Northwood, J. Electrochem. Soc. 146 (1999) 3591.